GEOPHYSICAL RESEARCH LETTERS, VOL. 35, L19607, doi:10.1029/2008GL034831, 2008

Non-linear alignment of El Niño to the 11-yr solar cycle

Warren B. White[1] and Zhengyu Liu[2]

Received 30 May 2008; revised 17 July 2008; accepted 13 August 2008; published 14 October 2008.

[1] El Nino/La Nina episodes represent warm/cool phases of 2- to 7-yr period El Nino-Southern Oscillation (ENSO) in the tropical Pacific ocean-atmosphere system. Modeling studies find ENSO self-excited or driven by ambient noise. Here we find most El Nino and La Nina episodes from 1900–2005 grouped into non-commuting pairs that repeat every ~11 yrs, aligned with rising and falling transition phases of the ~11-yr period quasi-decadal oscillation (QDO). These alignments arise from non-linear phase locking of 3rd and 5th harmonics near 3.6- and 2.2-yr to the 1st harmonic near 11-yr period. Here we find these alignments replicated in both coupled general circulation model and conceptual model driven by 11-yr solar forcing, wherein the solar-forced 1st harmonic initiates a non-linear cascade of higher odd harmonics that are phase-locked with the same alignments as observed. These solar-forced 3rd and 5th harmonics explain ~52% of inter-annual variance in the Nino-3 temperature index from 1900–2005.
Citation: White, W. B., and Z. Liu (2008), Non-linear alignment of El Niño to the 11-yr solar cycle, *Geophys. Res. Lett.*, *35*, L19607, doi:10.1029/2008GL034831.

1. Introduction

[2] El Nino/La Nina episodes represent warm/cool phases of the 2- to 7-yr period ENSO [*Philander*, 1990]. The ENSO is the mode(s) of inter-annual climate variability in the tropical Pacific delayed action/recharge oscillator (DAO) found self-excited or driven by internal noise [*Neelin et al.*, 1994; *Penland and Sardeshmukh*, 1995] in a variety of conceptual coupled models [*Graham and White*, 1988; *Jin*, 1997], intermediate coupled models [*Zebiak and Cane*, 1987; *Schopf and Suarez*, 1988], and general circulation coupled models [e.g., *Capotondi et al.*, 2006]. On the other hand, the QDO is the mode of quasi-decadal climate variability in the tropical Pacific DAO found driven by ~11-yr solar forcing in a conceptual model [*White et al.*, 2001] and in a coupled general circulation model [*White and Liu*, 2008].

[3] Here we find ENSO phase locked to the QDO, with most El Nino and La Nina episodes from 1900–2005 grouped into non-commuting pairs that repeat every ~11-yrs with rising and falling transition phases of the QDO. We also find these groupings and their alignments arise from non-linear forcing of 3rd and 5th harmonics near 3.6- and 2.2-yr period (i.e., ENSO signals) by the 1st harmonic near 11-yr period (i.e., QDO), all three odd harmonics governed by the same DAO with periods proportional to latitude of off-equatorial Rossby wave feedback [*White et al.*, 2003]. This yields a new paradigm for ENSO [*Wang and Picaut*, 2004], with El Nino and La Nina driven by the solar-forced QDO via non-linear processes in the tropical Pacific DAO.

2. Analysis of Observational and Model Data

[4] The local fractional variance spectrum [*Mann and Park*, 1999] of dominant spatial patterns of observed sea surface temperature (SST) variability [*Rayner et al.*, 2003] in the Pacific Ocean (40°S–40°N) from 1895–2005 (heavy curve in Figure 1a) is dominated by relatively narrow-band signals of the QDO near 11-yr period and of the ENSO near 5.5-, 4.4-, 3.6- 3.1-, 2.8-, and 2.2-yr period, as observed previously [*Allan*, 2000; *White and Tourre*, 2003]. The ~3.6- and ~2.2-yr ENSO signals are 3rd and 5th harmonics of the 1st harmonic QDO. Peaks in the amplitude time sequences of these odd harmonics (Figures 1d and 1e) of dominant SST spatial patterns (Figure 1b) are phase locked to one another from 1900–2000; i.e., peaks of the 3rd harmonic (5th harmonic) fluctuate nominally in phase (out of phase) with 7 of 9 peaks of the 1st harmonic.

[5] We propose that this phase locking occurs because 3rd and 5th harmonics are physically driven by the 1st harmonic via non-linear physical processes in the tropical Pacific DAO [*Lakshmanan and Rajaseekar*, 2003]. The 1st harmonic is driven by the ~11-yr solar cycle in a conceptual model of the tropical Pacific DAO [*White et al.*, 2001] and in the fully coupled ocean-atmosphere general circulation mode (FOAM) [*White and Liu*, 2008]. In the absence of 11-yr solar forcing, FOAM produced no QDO; but in its presence a model QDO was simulated with the same standing and propagating wave components as observed [*White et al.*, 2003]. Here we find solar-forced FOAM also simulating the 3rd and 5th harmonics of the model QDO (light curve in Figure 1a) near 3.6- and 2.2-yr period as observed (heavy curve in Figure 1a), again with the same standing and propagating wave components as observed [*White and Liu*, 2008]. Furthermore, peaks in corresponding amplitude time sequences (Figures 1f and 1g) of dominant SST spatial patterns (Figure 1c) are phase locked to one another over 100 model yrs; i.e., peaks of the 3rd harmonic (5th harmonic) fluctuate nominally in phase (~90° out of phase) with 7 of 9 peaks of the 1st harmonic, slightly different from that observed (Figures 1d and 1e).

[6] Visual alignments in observed and FOAM amplitude time sequences (Figures 1d–1g) are confirmed by forming 9-member composites (Figures 2a and 2b) referenced to the 9 peak warm phases of the ~11-yr signal that span respective 100-yr records. Peak warm phases of the ~11-yr QDO lag those of the ~3.6- and ~2.2-yr ENSO signals in observations (FOAM) by 0° ± 20° and 180° ± 20° (−30° ± 20° and 90° ± 20°) of the latter's phase respectively (Figures 2a and 2b). Subsequently, 9-member composites of their sum yield

[1]Scripps Institution of Oceanography, University of California San Diego, La Jolla, California, USA.
[2]Gaylord Nelson Institute for Environmental Studies, University of Wisconsin-Madison, Madison, Wisconsin, USA.

0094-8276/08/2008GL034831$05.00

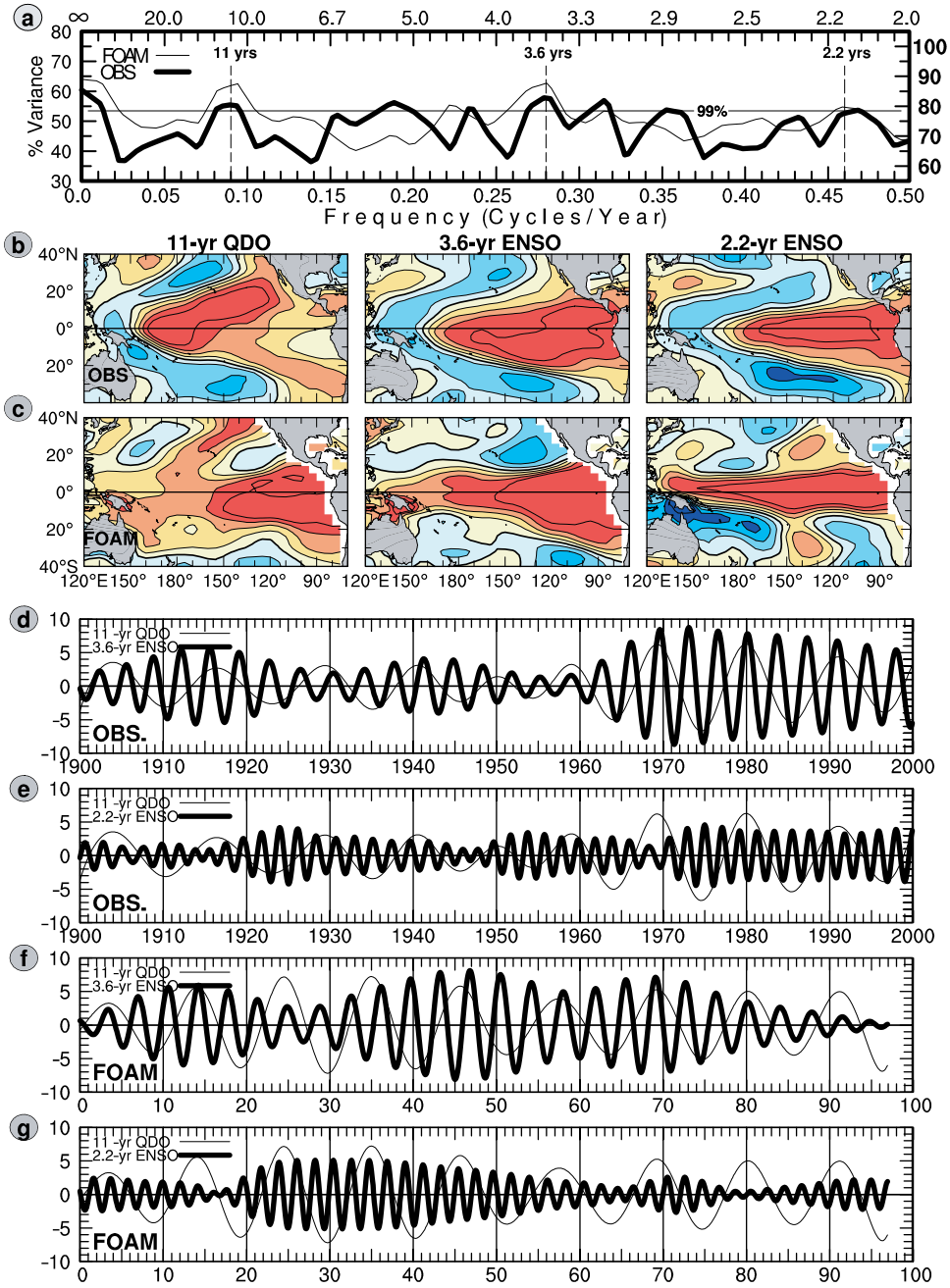

Figure 1. (a) Local fractional variance spectrum of multi-tapered method-singular value decomposition analysis of monthly Pacific SST variability (40°S–40°N) from solar-forced FOAM for model yrs 145–255 (light curve) and from observations for 1895–2005 (heavy curve), with 99% confidence level given by horizontal line. Dominant SVD spatial patterns of ~11-yr QDO, and ~3.6- and ~2.2-yr ENSO signals from (b) observations and (c) solar-forced FOAM. (d and e) Corresponding SVD amplitude time sequences of ~11-yr signal (light curve) superimposed on that of ~3.6-yr signal (dark curve in Figure 1d) and ~2.2-yr signal (dark curve in Figure 1e) for observations from 1900–2000. (f and g) Same as in Figures 1d and 1e, but over 100 yrs of solar-forced FOAM. Multiply the amplitude time sequence of each dominant SVD mode in Figures 1d–1g by normalized weights of its corresponding spatial pattern in Figures 1b and 1c to obtain its contribution to band-pass filtered SST variability at each grid point for any month. The time sequences of ~11-, ~3.6-, and ~2.2-yr variability at each grid point was obtained by band-pass filtering monthly records over 110 yrs with half-power points at 9- and 13-yr period, 3.4- and 3.8-yr period, and 2.1 and 2.3-yr period respectively [*Kaylor*, 1977], displayed over the middle 100 yrs.

characteristic quasi-decadal wave packets (Figure 2c) aligned with peak warm phase of the QDO, that in FOAM lagging that observed by ~6 months for reasons proposed in Section 3.

[7] Phase locking among odd harmonics also occurs in the Nino-3 SST index (5°S–5°N, 150°W–90°W), demonstrated by superimposing 9-member composites of the sum of ~3.6- and ~2.2-yr signals in the monthly Nino-3 SST

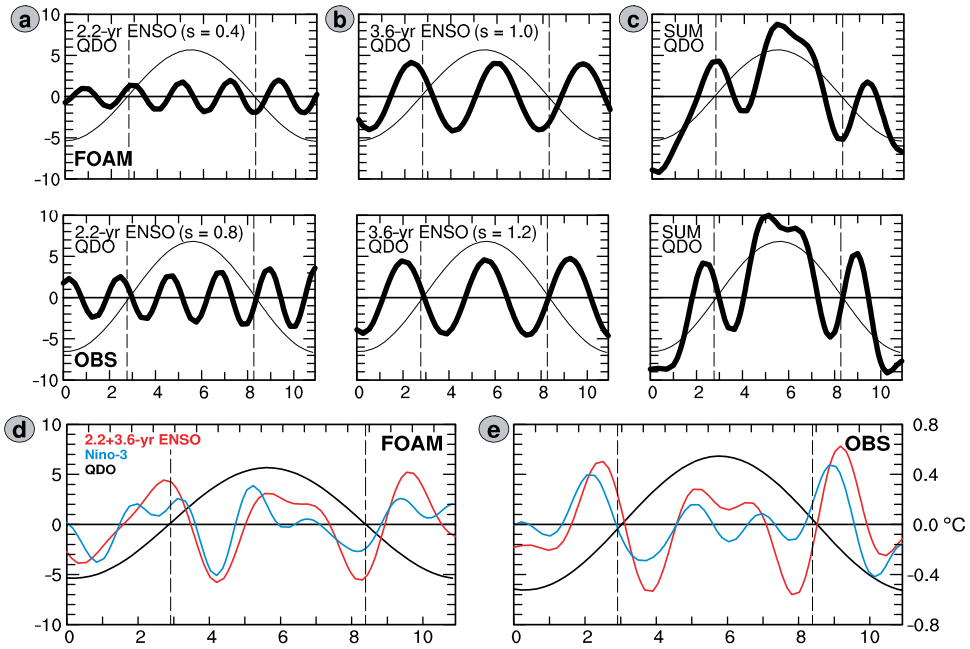

Figure 2. The 9-member composite averages of SVD amplitude time sequences referenced to the 9 peak warm phases of the ~11-yr signal during respective 100-yr records of observations and solar-forced FOAM: (a) ~11-yr QDO and ~2.2-yr ENSO signal; (b) ~11-yr QDO and ~3.6-yr ENSO signal; and (c) ~11-yr QDO and the sum of ~11-, ~3.6-, and ~2.2-yr signals. Ordinate (abscissa) gives relative magnitude (relative months) and "s" in upper left yields the standard error. (d and e) The same as in Figures 2a–2c but for the ~11-yr QDO (black curve), the sum of ~3.6- and ~2.2-yr signals in monthly Nino-3 SST indices (red curves), and for monthly Nino-3 SST indices (blue curves) over respective 100-yr records of FOAM and observations (OBS).

indices (red curves in Figure 2e) onto corresponding 9-member composites of monthly Nino-3 SST indices (blue curves in Figure 2e), both referenced to the 9 peak warm phases of the QDO that span respective 100-yr records in observations and FOAM (black curves in Figure 2e). A comparison finds dominant El Nino (E) and La Nina (L) episodes during the 20th Century grouped into non-commuting E-L and L-E pairs that tend to repeat every ~11-yrs (i.e., arising from constructive interference of the ~3.6- and ~2.2-yr signals), phase locked on average to rising and falling transition phases respectively of the QDO, with those in FOAM lagging those observed by ~6 months for reasons proposed below. These composites also find weaker/broader E (L) episodes (i.e., arising from destructive interference of the ~3.6- and ~2.2-yr signals) phase-locked on average with peak warm (cool) phases of the QDO.

3. Solutions of a Conceptual Model of Tropical Pacific Climate Variability

[8] To begin understanding the source of these odd harmonics, we examine a familiar non-linear conceptual model for tropical Pacific DAO [*Jin*, 1997] driven by 11-yr solar forcing; i.e.,

$$\begin{aligned} dh/dt &= -T + \varepsilon, \\ dT/dt + \gamma T &= \left(h + bh^3\right) + S\cos(t). \end{aligned} \tag{1}$$

Accordingly, "T" in Equation (1a) represents positive upper ocean temperature anomalies in the eastern equatorial Pacific Ocean driving shallow thermocline depth anomalies (h) off the equator near 15° latitude via T-induced cyclonic wind stress curl anomalies and ambient noise (ε). And, "h" in Equation (1b) represents western boundary Rossby wave reflection of its counterpart in the first equation, providing a negative feedback to the T tendency in the eastern equatorial ocean via a non-linear thermocline displacement [i.e., $(h + bh^3)$], together with 11-yr solar cosine forcing. Instantaneous positive feedback from T-induced zonal surface wind stress along the equator is neglected.

[9] Equation (1) has time scaled by frequency (ω) of 11-yr solar forcing, yielding unit coefficient ($\omega_O/\omega = 1$) modifying the linear restoring force (h), the 11-yr quasi-decadal normal mode (ω_O) presumed to exist in the absence of solar forcing [*Capotondi and Alexander*, 2001]. This scaling non-dimensionalizes the dissipation coefficient (γ) as well, leaving variables "T" and "h" in units of tenths°C and meters, respectively. Non-linear delayed negative feedback ($h + bh^3$) represents thermocline displacement, its vertical gradient separating near-surface and deep-ocean mixed layers proportional to "b".

[10] Equation (1) is also the well-known non-linear Duffing oscillator, wherein cubic non-linear restoring forces produce a periodic frequency-jump phenomenon (i.e., a form of deterministic chaos) responsible for the wave packet response in periodic externally forced non-linear springs [*Lakshmanan and Rajaseekar*, 2003]. We solve Equation (1) for T and h for two dissipation coefficients (γ = 1.0 and 0.33) and b = 3, S = 8 as rationalized below, finding the characteristic wave packet solution portrayed in the time sequence of T (Figures 3a and 3b, left). Corresponding

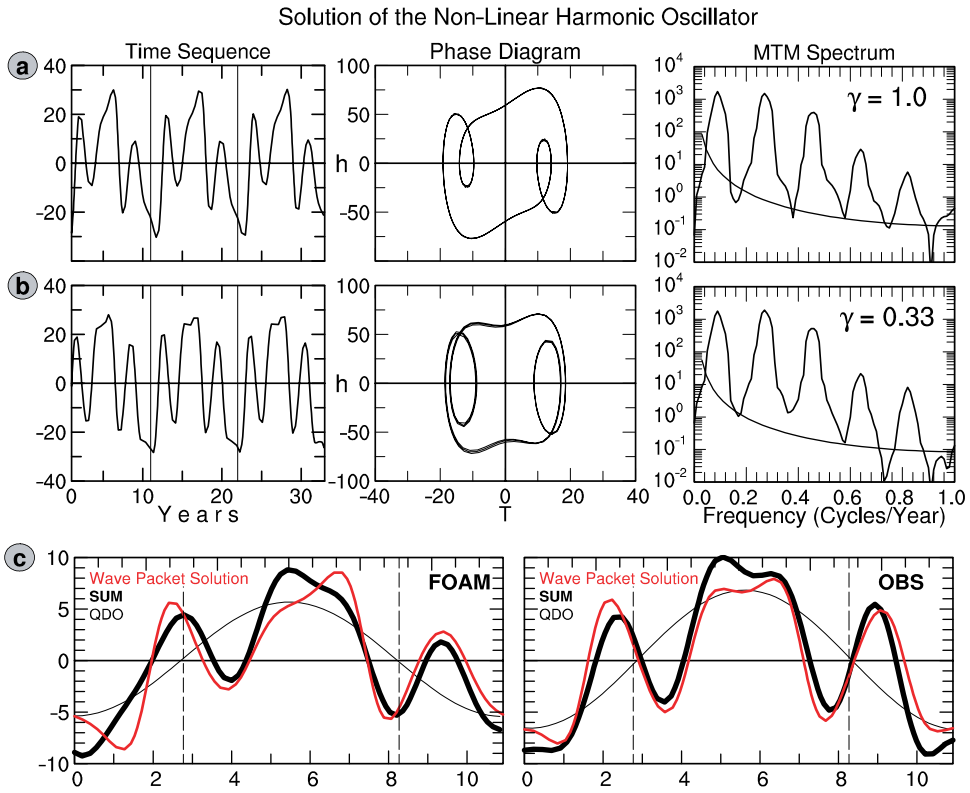

Figure 3. (a) The wave packet solution for T in the non-linear conceptual model of the tropical Pacific DAO in Equation (1) for $\gamma = 1.0$, displaying the time sequence of T (tenths °C), the phase diagram of T (tenths°C) versus h (meters), and the MTM power spectrum [*SSA-MTM Group*, 2003] of T, with 99% confidence given by curved line. (b) The same as in Figure 3a but for $\gamma = 0.33$. (c) (left) The wave packet solution for T in Figure 3a (red curve) superimposed on 9-member composite averages of the SVD amplitude time sequences of the ~11-yr signal in SST variability (light black curve) and of the sum of ~11-, ~3.6-, and ~2.2-yr signals (heavy black curve) from solar-forced FOAM (repeated from Figure 2c, top) and (right) the same as in Figure 3c, left, but for T in Figure 3b (red curve) superimposed on 9-member composite averages from observations (repeated from Figure 2c, bottom). Ordinate (abscissa) gives relative magnitude (relative months).

phase diagrams of T versus h (Figures 3a and 3b, middle) displays a large elliptical attractor representing the 1st harmonic, with smaller single-orbit attractors in left and right hemispheres deriving from constructive interference of 3rd and 5th harmonics in the corresponding power spectrum (Figures 3a and 3b, right). Superimposing the non-linear wave packet solution for $\gamma = 1.0$ and 0.33 onto FOAM and observed wave packets respectively (Figure 3c, left and right) finds them nearly identical, with E-L and L-E pairs for $\gamma = 1.0$ lagging those for $\gamma = 0.33$ by ~6 months. This lag derives from dissipation in coarse-grid FOAM being larger than in the real ocean-atmosphere system.

[11] Equation (1) yields this wave packet solution across a broad range of model parameters, from relatively sharp thermocline (i.e., b = 40) and weak solar forcing (i.e., S = 2 tenths°C) to relatively broad thermocline (i.e., b = 3) and strong solar forcing (i.e., S = 8 tenths°C), with greater non-linearity and/or external forcing intensifying the higher odd harmonics. We choose this latter parameter group, where $S = S_O/(\rho_O C_{PO} H\omega) \approx 8$ tenths°C, wherein anomalous solar insolation S_O of 3 Wm^{-2} heats the near surface mixed layer of depth scale H ≈ 50 m [*White et al.*, 1997]. This estimate for S_O represents the root-mean-square of regional surface solar insolation anomalies observed across the tropical Pacific Ocean during peak ~11-yr solar forcing [*Meehl et al.*, 2008]. Whilst this is an order of magnitude larger than the amplitude of peak ~11-yr solar radiative forcing of ~0.3 Wm^{-2} at the top of the tropical atmosphere [*Lean et al.*, 2005], both *van Loon et al.* [2007] and *Meehl et al.* [2008] find the latter amplified by an order of magnitude in relatively cloud-free domains via strong positive feedbacks from regional vertical-horizontal circulation cells in the troposphere.

[12] In Equation (1), substituting the solar-forced 1st harmonic solution for h [i.e., cos(t)] into the cubic negative feedback term yields $b[\cos(t)]^3 = b[3/4\cos(t) + 1/4\cos(3t)]$, introduces an additional negative feedback for the 3rd harmonic. Repeating this substitution with cos(3t) at the next level of approximation generates negative feedbacks for the 5th and 7th harmonics, and so on. Thus, the solar-forced QDO forces the ~3.6-yr ENSO signal, which in turn forces the ~2.2-yr ENSO signal, and so on, leading to a non-linear cascade of higher odd harmonic generation (Figures 3a and 3b, right), all instigated by the 11-yr solar forcing.

4. Discussion and Conclusions

[13] The sum of solar-forced ~3.6- and ~2.2-yr harmonics in the observed monthly Nino-3 SST index (red curve,

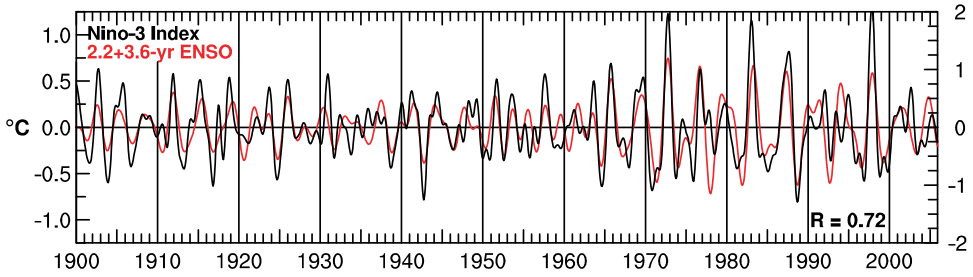

Figure 4. Superposing the sum of ~3.6- and ~2.2-yr signals from the observed monthly Nino-3 SST index (red curve) on the inter-annual Nino-3 SST index (for periods >1.0 yr) (black curve) from 1900–2005, with cross-correlation (R) in lower right corner.

Figure 4) explains ~52% of inter-annual variance for periods >1 yr (black curve, Figure 4), significant at >99% confidence for 32 degrees of freedom, producing peaks that align with ~75% (i.e., 24 of 32) of El Nino episodes from 1900–2005, with ~6 false positives. These odd harmonics dominate other ENSO signals (heavy curve in Figure 1a) and noise in explaining inter-annual variance in the Nino-3 SST index.

[14] This also finds 18 of ~32 El Nino episodes from 1900-2005 grouped into the E-L (L-E) pairs in 1900, 1912, 1926, 1937–38, 1948, 1957–58, 1966, 1976–77, 1987, 1998 (1908, 1919, 1933, 1944, 1953, 1962–63, 1973, 1983, 1995, 2005) that tend to straddle rising (falling) transition phases of the QDO, with 8 additional E episodes (generally weaker) in 1903, 1915, 1931, 1941, 1969, 1980, 1991–92, and 2002 nominally aligned with peak phases of the QDO, as indicated in the composites (Figures 2c–2e). This alignment was better from 1900–1920 and 1960–2005 (1920–1960) when amplitude of the QDO (Figure 1d) and of ~11-yr solar forcing [*White et al.*, 1997] was higher (lower), this latter epoch finding E and L notably weaker as well (black curve, Figure 4), consistent with multi-decadal amplitude modulation of ENSO in evolutive spectra [*Allan*, 2000].

[15] Wave packet responses to 11-yr solar forcing in FOAM and the conceptual model are similar (Figure 3c). However, the response to ambient noise in the conceptual model yields a weak QDO but no higher odd harmonics, while in FOAM it yields no QDO but weak higher odd harmonics [*Liu et al.*, 2000], Thus, higher odd harmonics in the observations may be self-excited or driven by ambient noise, as in FOAM and other general circulation models, but intensified by, and synchronized to, the solar-forced QDO.

[16] Solar-forced FOAM generated ~11-, ~3.6-, and ~2.2-yr harmonics, each harmonic governed by the same tropical Pacific DAO, with period proportional to latitude of off-equatorial Rossby wave reflection [*White and Liu*, 2008] as observed [*Graham and White*, 1988; *Graham et al.*, 1990; *White et al.*, 2003]. The ~11-yr solar forcing excited the 11-yr QDO in this tropical Pacific DAO, while internal non-linear processes therein allow the solar-forced QDO to drive or synchronize the ~3.6- and ~2.2-yr ENSO signals. It remains to determine whether these non-linear processes are the same as those in Equation (1).

[17] **Acknowledgments.** Warren White is supported by NASA and UCSD. Zhengyu Liu is supported by NOAA, DOE, and UWM.

References

Allan, R. (2000), ENSO and climatic variability in the last 150 years, in *El Niño and the Southern Oscillation: Multiscale Variability, Global and Regional Impacts*, edited by H. F. Diaz and V. Markgrav, pp. 3–56, Cambridge Univ. Press, Cambridge, U.K.

Capotondi, A., and M. A. Alexander (2001), Rossby waves in the tropical North Pacific and their role in decadal thermocline variability, *J. Phys. Oceanogr.*, *31*, 3496–3515.

Capotondi, A., A. Wittenberg, and S. Masina (2006), Spatial and temporal structure of tropical Pacific interannual variability in 20th century coupled simulations, *Ocean Modell.*, *15*, 274–298.

Graham, N. E., and W. B. White (1988), The El Niño cycle: A natural oscillator of the Pacific ocean-atmosphere system, *Science*, *240*, 1293–1302.

Graham, N. E., W. B. White, and A. Pares-Sierra (1990), Low frequency ocean-atmosphere interactions in the tropical Pacific, in *Air-Sea Interaction in the Tropical Western Pacific*, edited by C. Jiping and J. Young, pp. 457–484, China Ocean Press, Beijing.

Jin, F.-F. (1997), An equatorial ocean recharge paradigm for ENSO. Part I: Conceptual model, *J. Atmos. Sci.*, *54*, 811–829.

Kaylor, R. E. (1977), *Filtering and Decimation of Digital Time Series, Tech. Rep. Note BN 850*, 14 pp., Inst. of Phys. Sci, and Technol., Univ. of Md., College Park.

Lakshmanan, M., and S. Rajaseekar (2003), *Nonlinear Dynamics: Integrability, Chaos, and Patterns*, 619 pp., Springer, New York.

Lean, J., G. Rottman, J. Harder, and G. Kopp (2005), SORCE contributions to new understanding of global change and solar variability, *Sol. Phys.*, *230*, 27–53.

Liu, Z., J. Kutzbach, and L. Wu (2000), Modeling climatic shift of El Nino variability in the Holocene, *Geophys. Res. Lett.*, *27*, 2265–2268.

Mann, M., and J. Park (1999), Oscillatory spatio-temporal signal detection in climate studies: A multiple-taper spectral domain approach, *Adv. Geophys.*, *41*, 1–131.

Meehl, G. A., J. M. Arblaster, G. Branstator, and H. Van Loon (2008), A coupled air-sea response mechanism to solar forcing in the Pacific region, *J. Clim.*, *21*, 2883–2897.

Neelin, J. D., M. Latif, and F. F. Jin (1994), Dynamics of coupled ocean-atmosphere models: The tropical problem, *Annu. Rev. Fluid Mech.*, *26*, 617–659.

Penland, C., and P. Sardeshmukh (1995), The optimal growth of the tropical sea surface temperature anomalies, *J. Clim.*, *8*, 1999–2024.

Philander, S. G. (1990), *El Niño, La Niña, and the Southern Oscillation*, 293 pp., Academic Press, San Diego, Calif.

Rayner, N., et al. (2003), Global analyses of sea surface temperature, sea ice, and night marine air temperature since the late nineteenth century, *J. Geophys. Res.*, *108*(D14), 4407, doi:10.1029/2002JD002670.

Schopf, P. S., and M. J. Suarez (1988), Vacillations in a coupled ocean-atmosphere model, *J. Atmos. Sci.*, *45*, 549–566.

SSA-MTM Group (2003), SSA-MTM Toolkit 4.1, user's guide, report, Dep. of Atmos. Sci., Univ. of Calif., Los. Angeles.

van Loon, H., J. A. Meehl, and D. J. Shea (2007), Coupled air-sea response to solar forcing in the Pacific region during northern winter, *J. Geophys. Res.*, *112*, D02108, doi:10.1029/2006JD007378.

Wang, C., and J. Picaut (2004), Understanding ENSO physics—A review, in *Earth's Climate: The Ocean–Atmosphere Interaction*, *Geophys. Monogr. Ser.*, vol. 147, pp. 21–48, AGU, Washington, D. C.

White, W. B., and Z. Liu (2008), Resonant excitation of the quasi-decadal oscillation by the 11-year signal in the Sun's irradiance, *J. Geophys. Res.*, *113*, C01002, doi:10.1029/2006JC004057.

White, W. B., and Y. M. Tourre (2003), Global SST/SLP waves during the 20th century, *Geophys. Res. Lett.*, *30*(12), 1651, doi:10.1029/2003GL017055.

White, W. B., J. Lean, D. Cayan, and M. Dettinger (1997), Response of global upper ocean temperature to changing solar irradiance, *J. Geophys. Res.*, *102*, 3255–3266.

White, W. B., M. Dettinger, and D. Cayan (2001), Global average upper-ocean temperature response to changing solar irradiance: Exciting the internal decadal mode, in *SOLSPA 2000 Proceedings of 1st Solar Space Weather*, edited by A. Wilson, pp. 125–133, Publ. Div., Eur. Space Agency, Noordwijk, Netherlands.

White, W. B., Y. M. Tourre, M. Barlow, and M. Dettinger (2003), A delayed action oscillator shared by biennial, interannual, and decadal signals in the Pacific basin, *J. Geophys. Res.*, *108*(C3), 3070, doi:10.1029/2002JC001490.

Zebiak, S. E., and M. A. Cane (1987), Model El Niño–Southern Oscillation, *Mon. Weather Rev.*, *115*, 2262–2278.

Z. Liu, Gaylord Nelson Institute for Environmental Studies, University of Wisconsin-Madison, Madison, WI 53706-1695, USA.

W. B. White, Scripps Institution of Oceanography, University of California San Diego, 9500 Gilman Drive, La Jolla, CA 92093-0230, USA. (wbwhite@ucsd.edu)